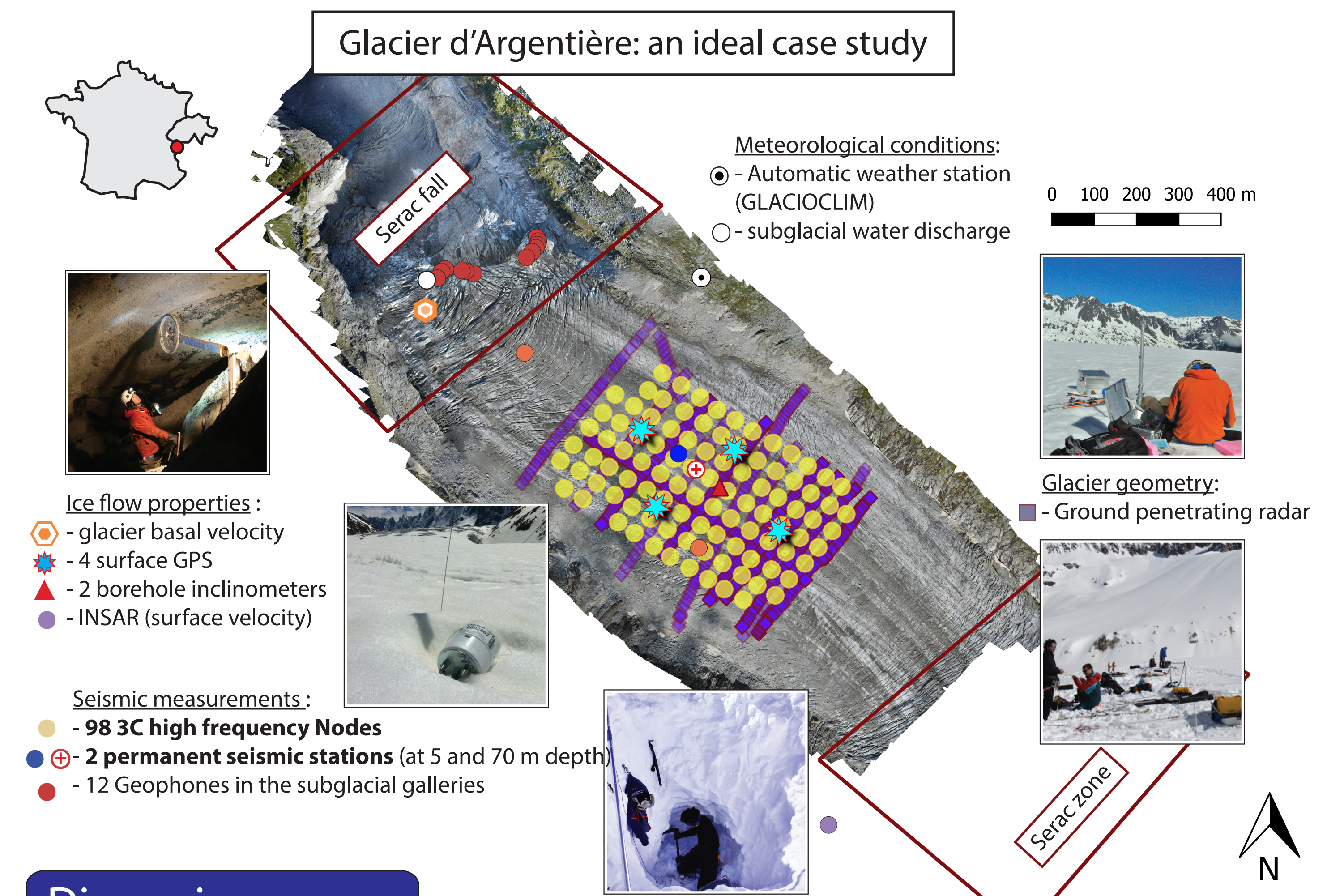




## Experimental setup

**Glacier dynamics** regulates the advection of ice towards lower elevations with higher temperature and melt rates, and thus controls the fresh water supply to populations for mountain glaciers and sea level rise for ice sheets. The **RESOLVE-Argentière** project aims at:  
- providing finely resolved observations of **glacier process** from the use of **dense geophysical array**.  
- using the observations to **improve physical laws** in theoretical ice-flow models.



## Seismic and glaciological context

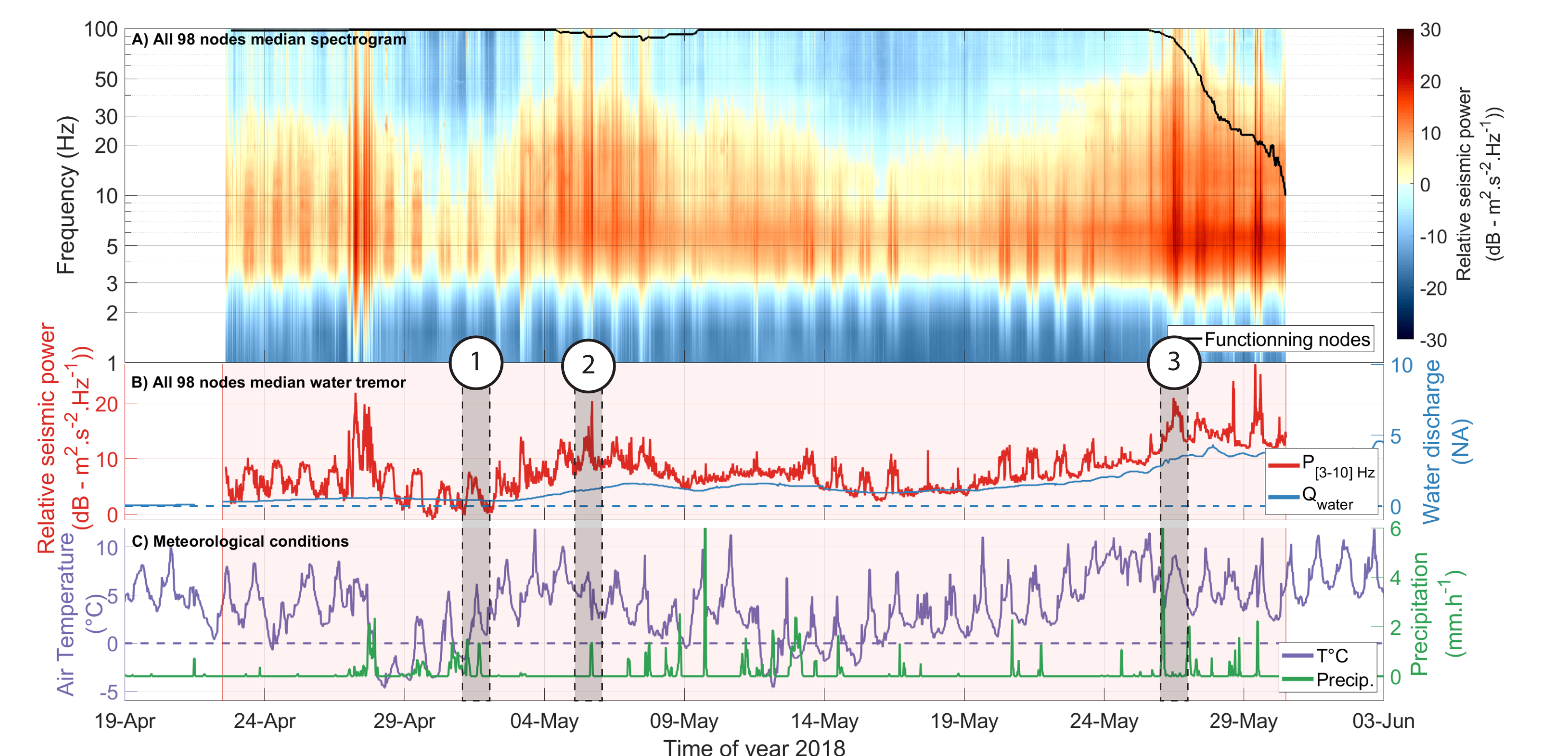


Figure 2: Time series of physical quantities measured during the RESOLVE-Argentière project. (a) Median seismic power taken over the 98 nodes. (b) Median seismic power assembled from the 98 nodes as averaged in the [3-10] Hz frequency range (red line) and subglacial water discharge (blue line). (c) Surface air temperature (purple line) and precipitations (green line). Numbers refers to Fig. 12

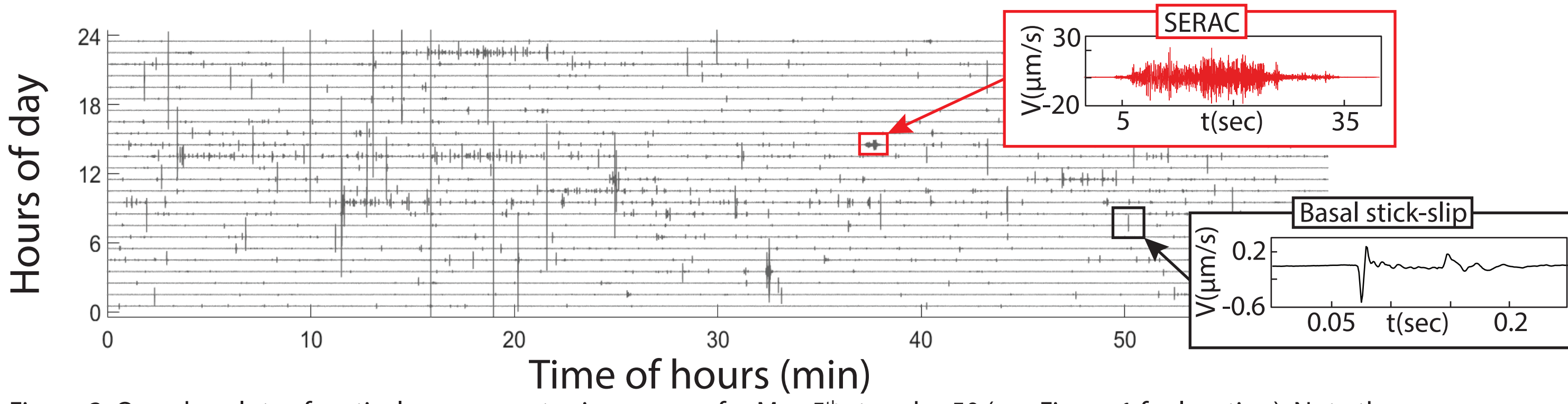


Figure 3: One-day plots of vertical-component seismograms for May 5<sup>th</sup> at nodes 50 (see Figure 1 for location). Note the numerous impulsive events whose amplitudes are above the background noise.

## Event detection and location method

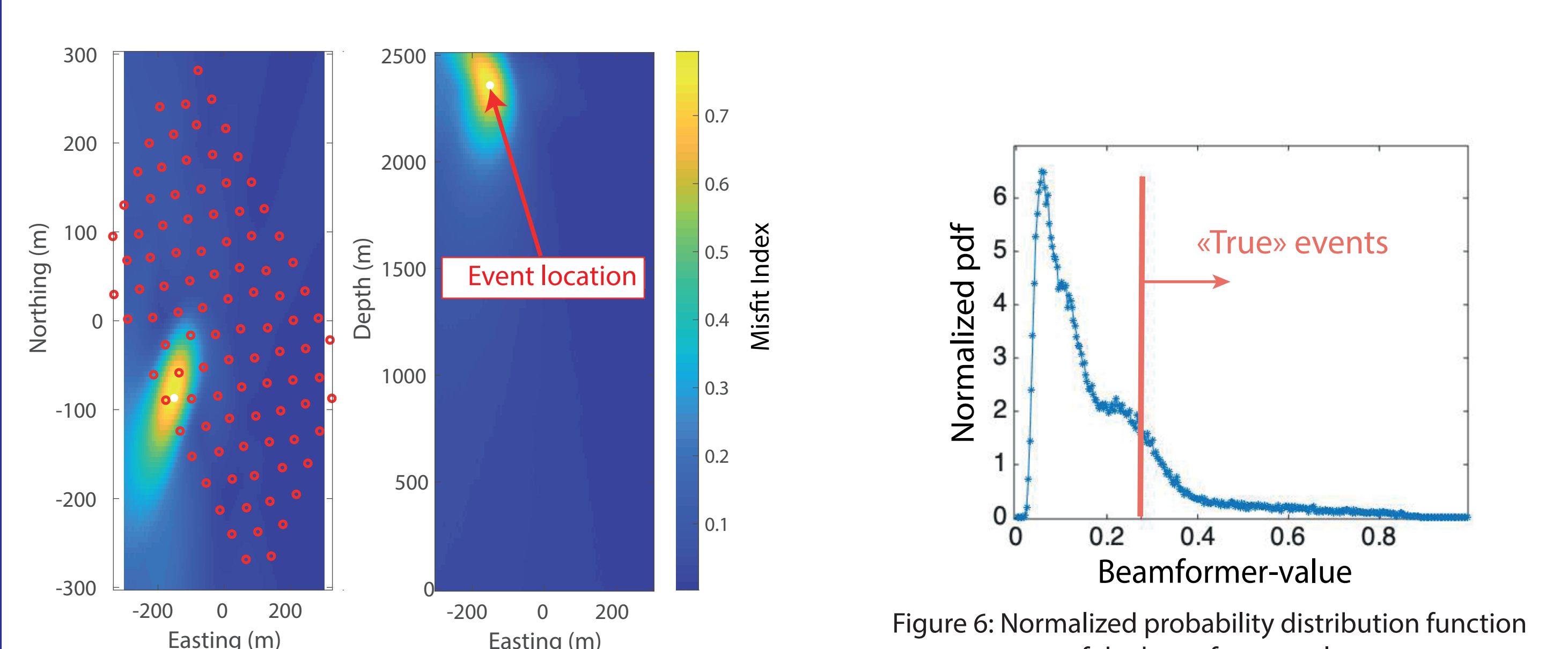
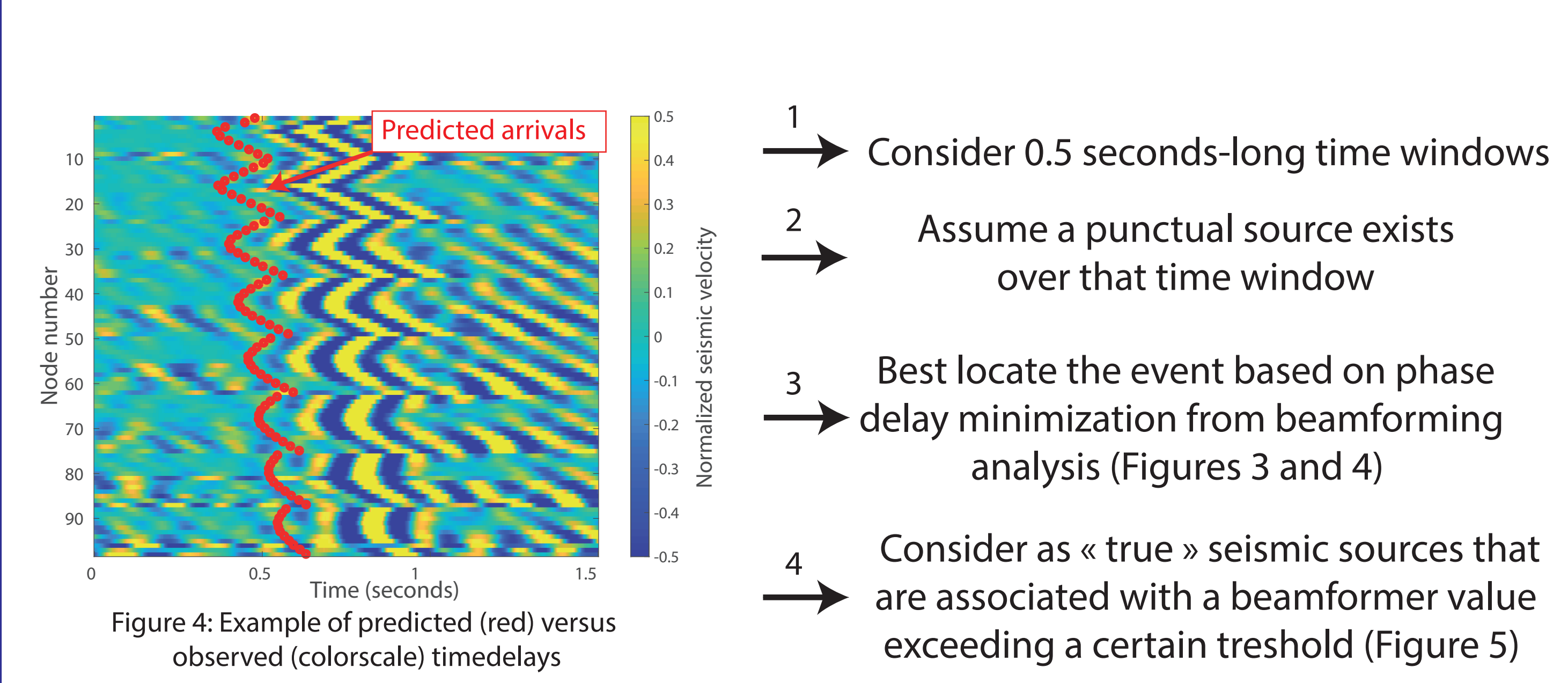


Figure 5: Example of focal footprint associated with an event of beamformer value equal to 0.53

## Dispersion curves

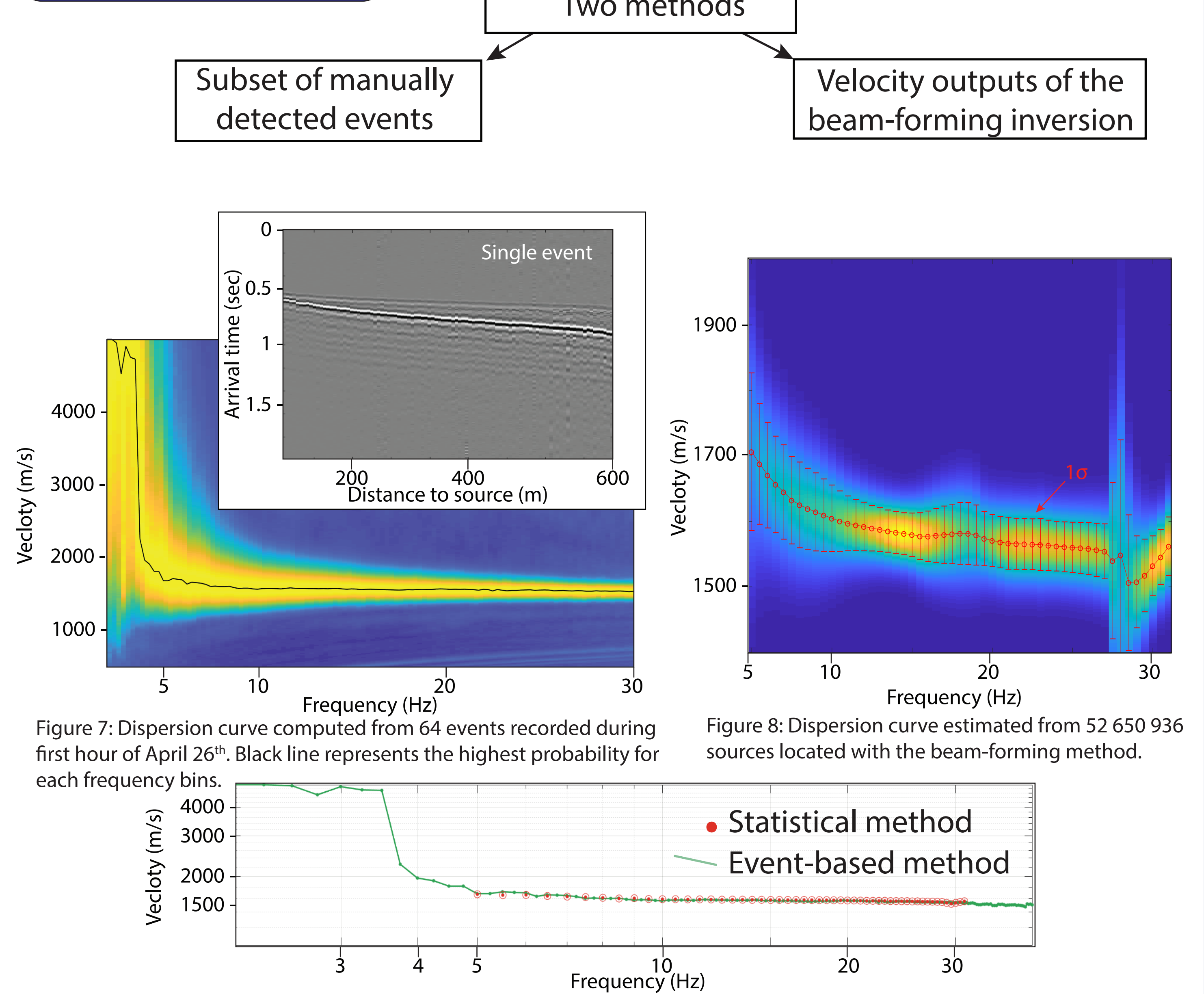


Figure 7: Dispersion curve computed from 64 events recorded during first hour of April 26<sup>th</sup>. Black line represents the highest probability for each frequency bins. Figure 8: Dispersion curve estimated from 52 650 936 sources located with the beam-forming method. Figure 9: Comparison between the two methods to compute the dispersion curve.

## Spatio-temporal dynamics of punctual sources

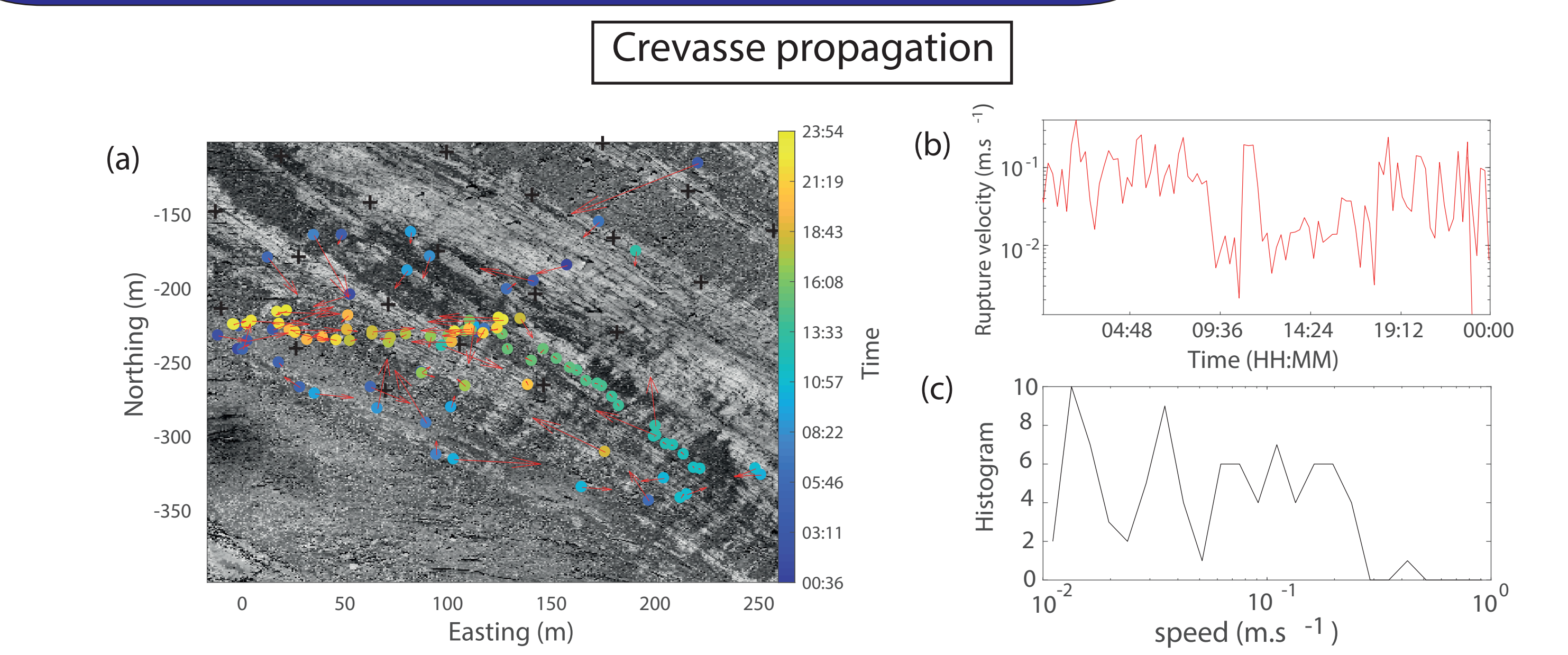


Figure 10: Rupture propagation of a crevasse as observed on April 26 (using 17 Hz frequency waveforms). (a) Localization of rupture events through time (see colorscale). Red arrows indicate velocity vectors. (b) Rupture velocity as a function of time throughout the day. (c) Histogram of rupture velocities.

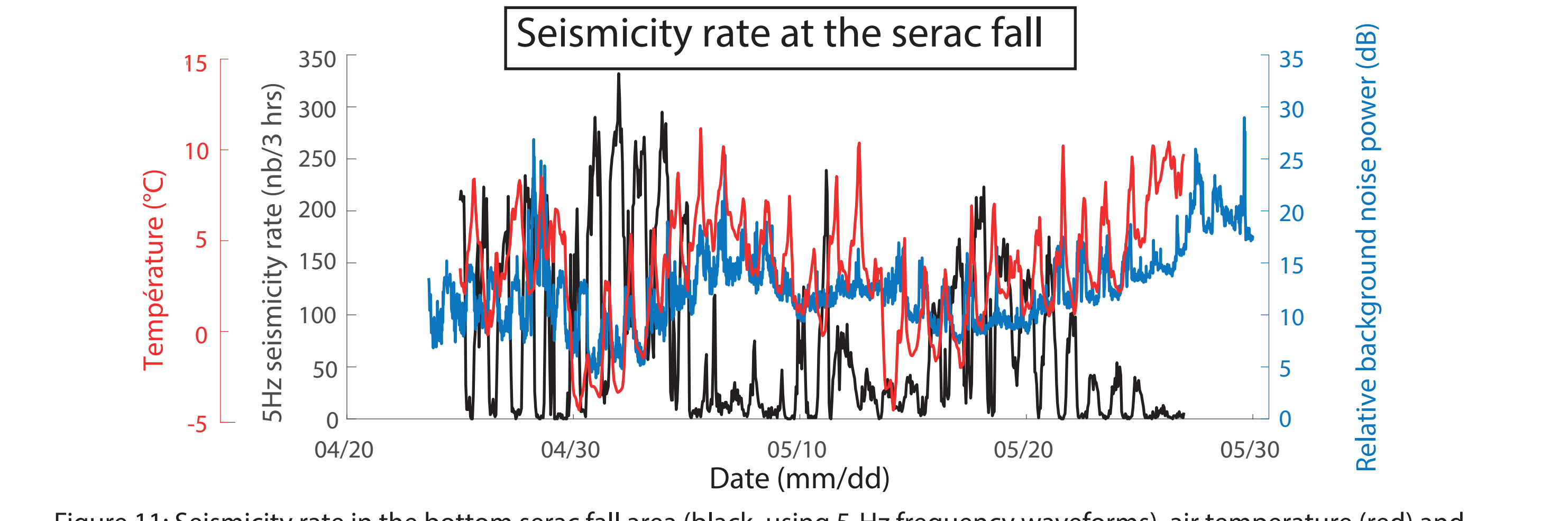


Figure 11: Seismicity rate in the bottom serac fall area (black, using 5-Hz frequency waveforms), air temperature (red) and background seismic noise power (blue) as a function of time.

## Seismic amplitudes

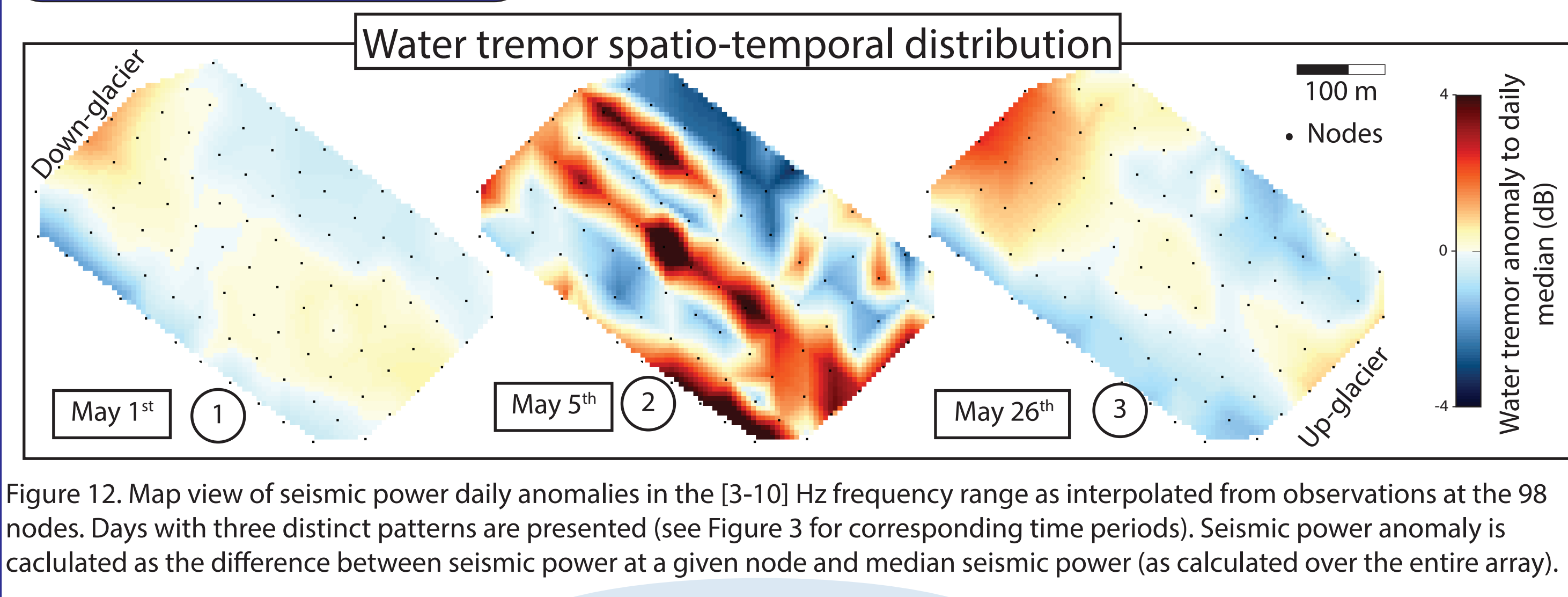


Figure 12: Map view of seismic power daily anomalies in the [3-10] Hz frequency range as interpolated from observations at the 98 nodes. Days with three distinct patterns are presented (see Figure 3 for corresponding time periods). Seismic power anomaly is calculated as the difference between seismic power at a given node and median seismic power (as calculated over the entire array).

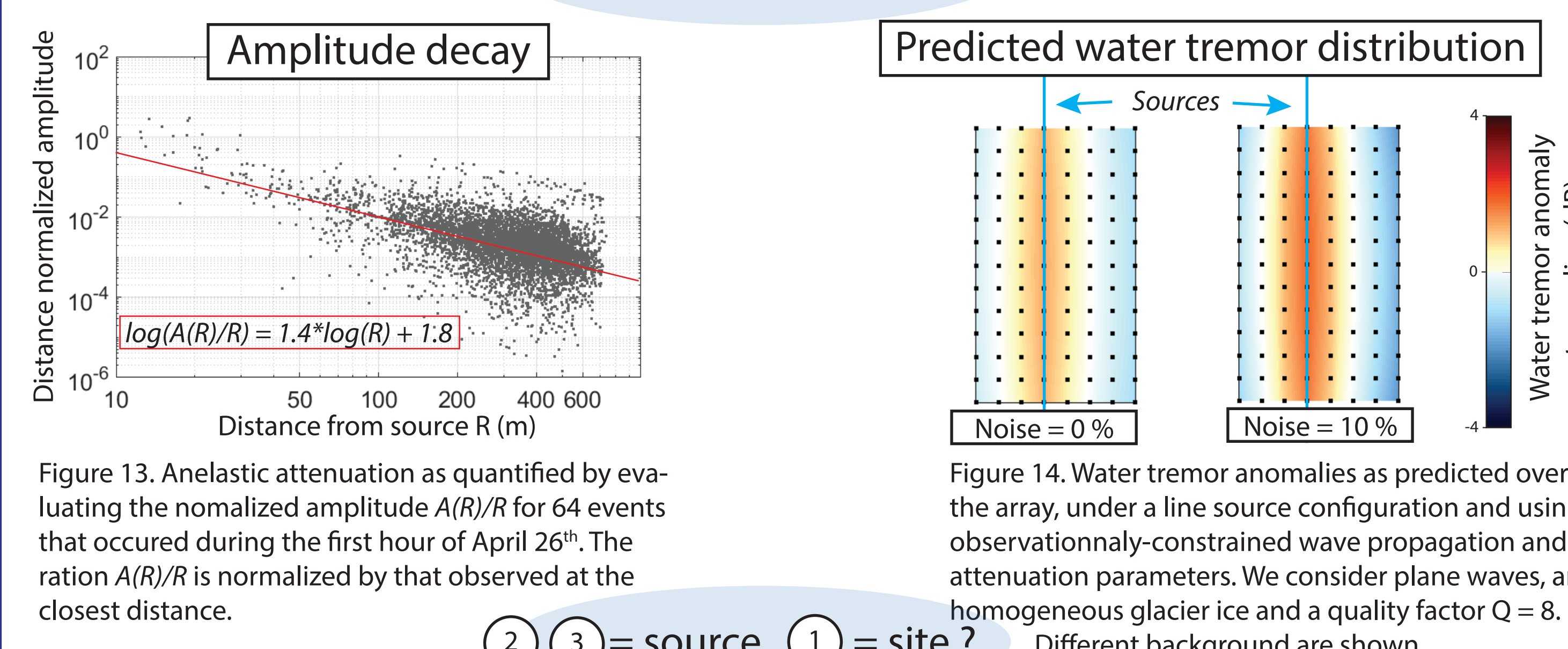


Figure 13: Anelastic attenuation as quantified by evaluating the normalized amplitude  $A(R)/R$  for 64 events that occurred during the first hour of April 26<sup>th</sup>. The ratio  $A(R)/R$  is normalized by that observed at the closest distance. Figure 14: Water tremor anomalies as predicted over the array, under a line source configuration and using observationally-constrained wave propagation and attenuation parameters. We consider plane waves, an homogeneous glacier ice and a quality factor  $Q = 8$ . Different background are shown.